Conformation of Pleionomers of α-Aminoisobutyric Acid[1]

Claudio Toniolo,*[2a] Gian Maria Bonora,[2a] Vincenzo Barone,[2b] Alfonso Bavoso,[2b] Ettore Benedetti,[2b] Benedetto Di Blasio,[2b] Patrizio Grimaldi,[2b] Francesco Lelj,[2b] Vincenzo Pavone,[2b] and Carlo Pedone[2b]

Biopolymer Research Centre, CNR, Institute of Organic Chemistry, University of Padua, 35131 Padua, Italy, and Department of Chemistry, University of Naples, 80134 Naples, Italy. *Received August 6, 1984*

ABSTRACT: The IR absorption and ^{1}H NMR analysis of the preferred conformation of monodisperse Z-(Aib)$_n$-O*t*Bu (Z = (benzyloxy)carbonyl, O*t*Bu = *tert*-butoxy, Aib = α-aminoisobutyric acid; n = 1–12) strongly indicates the formation of fully developed stable 3_{10}-helices for the higher (n = 8–12) homooligomers (*pleionomers*). This experimental study was performed in the solid state as well as in deuteriochloroform solution, in the latter case as a function of concentration, temperature, and addition of dimethyl sulfoxide and the free radical Tempo. A picture of the mode of self-association of the helical structures has also been obtained. A detailed theoretical study of Aib *N*-acetyl-*N*′-methyl amide by conformational energy computations indicates that the fully extended structure is less stable than the helical structures, irrespective of the actual value of the N–C$^\alpha$–C′ valence angle.

Introduction

Aib (α-aminoisobutyric acid or α,α-dimethylglycine) is the prototype of α,α-dialkylated α-amino acids. Conformational energy computations of Ac-Aib-NHMe (Ac = acetyl; NHMe = methylamino) show that the presence of two methyl groups on the C$^\alpha$ carbon imposes a marked restriction on the available conformational space.[3-17] Folded (helical) structures of the 3_{10} ($\varphi = \pm 60°$, $\psi = \pm 30°$) and α ($\varphi = \pm 55°$, $\psi = \pm 45°$) types are significantly more stable than extended ($\varphi \approx \psi \approx 180°$) structures. Conversely, the energy difference between the 3_{10}- and α-helical structures is small.

A few years ago in their calculations on Ac-Aib-NHMe and poly(Aib)$_n$, Venkataram Prasad and Sasisekharan took into account the nonplanar distortion of the peptide unit. For the value $\Delta\omega = +6°$, experimentally observed in the X-ray diffraction structures of oligopeptides containing the Aib–Aib sequence, a modified α-helix ($\varphi = \pm 55°$, $\psi = \pm 60°$) called the α′-helix, was found to be the most stable structure.[16,17] More recently, Paterson et al.[12] demonstrated that the preferred helical conformation of Ac-(Aib)$_n$-NHMe (n = 1–3) is also sensitive to the molecular geometry (in particular to the valence angles between the four substituents on the tetrahedral C$^\alpha$ atom) assigned to this residue: a tetrahedral symmetric geometry for these substituents favors the α-helix, whereas an asymmetric geometry, derived from published X-ray diffraction structures, favors the 3_{10}-helix. Interestingly, in the early 1960s, Blout and Fasman,[18] and Elliott et al.,[19] independently, from simple analysis of molecular models were able to show that unfavorable steric interactions are more significant in the α-helix of poly(Aib)$_n$ than in the 3_{10}-helix.

Experimental investigations of poly(Aib)$_n$ were carried out on *polydisperse* materials (prepared from *N*-carboxyanhydride polymerization[20-25]). X-ray diffraction powder photographs and unpolarized IR absorption results were originally interpreted in terms of an α-helix,[26,27] whereas more recent electron-diffraction photographs and polarized IR absorption data of oriented specimens produced evidence that the 3_{10}-helix is the preferred conformation.[28,29] A vibrational analysis of the normal modes of poly(Aib)$_n$ in both the α- and 3_{10}-helices showed significant differences only in the 300–900-cm^{-1} region: a comparison of observed with calculated frequencies supported the view of the occurrence of the 3_{10}-helical structure for the polypeptide.[30]

Published experimental investigations on *monodisperse* Aib homooligomers are limited to the pentamer level. Single-crystal X-ray diffraction data of protected (Aib)$_n$ (n = 1–5) homopeptides are indicative of the onset of folded structures in the solid state.[1,14,31-43] In addition, the observed intramolecular N—H···O=C H-bonding schemes of the trimer, tetramer, and pentamer are compatible with the occurrence of (incipient) 3_{10}-helices.[31-34,37,39] Solution IR absorption and ^{1}H NMR studies of fully protected (Aib)$_n$ (n = 1–5) homopeptides[32,44-52] strongly support the view that the intramolecular H bonds of the C_{10} type,[53] characteristic of the 3_{10}-helix, are first formed at the trimer level.

However, it is generally agreed that the conformational properties of low-molecular-weight oligomers ($n \leq 5$) are often not representative of the corresponding pleionomers (the monodispersed higher homologues having a main-chain length greater than the critical chain length for the onset of the ordered structure typical of the related homopolymer) and high-molecular-weight polymers due to the predominance of end-group effects operative in the former.[54] Therefore, to get a clear-cut answer to the problem of the conformation adopted by high-molecular-weight poly(Aib)$_n$, we have extended the investigation of the complete, strictly monodispersed, fully protected Z-(Aib)$_n$-O*t*Bu (Z = (benzyloxy)carbonyl; O*t*Bu = *tert*-butoxy) homooligopeptides series to n = 12. In addition to the synthetic details, in this paper we report the results of a conformational analysis in the solid state as well as in $CDCl_3$ solution, in the latter case as a function of concentration, temperature, and addition of dimethyl sulfoxide (Me_2SO) and the free radical 2,2,6,6-tetramethylpiperidinyl-1-oxy (Tempo).

In order to complete the picture of the conformational characteristics of Aib oligomers, we have, finally, performed detailed conformational energy computations of Ac-Aib-NHMe, including optimization of the N–C$^\alpha$–C′ angle, whose value is strongly conformation dependent.[15] The results obtained are also expected to help our understanding of the conformational preferences of the membrane-active, channel-forming, Aib-rich peptide (*peptaibol*) antibiotics.[13,14,40,55-61]

Experimental Section

Synthesis of Peptides. Z-(Aib)$_n$-O*t*Bu (n = 3–12) were synthesized from the appropriate *N*-[(benzyloxy)carbonyl]oxazolones (n = 2–6)[34,62,63] and H-(Aib)$_n$-O*t*Bu (n = 1–6)[63] in anhydrous acetonitrile under reflux as described by Jones et al.[63] Interestingly, the analytically pure, highest oligomers (n = 6–12) were easily obtained by filtration of the reaction mixtures at room temperature. The C-deprotected derivatives Z-(Aib)$_n$-OH (n = 2–6) were prepared from the corresponding *tert*-butyl esters by using trifluoroacetic acid.[62-64] Z-(Aib)$_n$-O*t*Bu (n = 1, 2),[63,65] Z-

0024-9297/85/2218-0895$01.50/0

Table I
Summary of Analytical Data and Physical Properties of the Z-(Aib)$_n$-O*t*Bu (n = 7–12) Homooligomers[a]

	C, %		N, %		H, %		
n	calcd	found	calcd	found	calcd	found	mp,[b] °C
7	59.8	59.6	8.2	8.3	12.2	12.3	229–230
8	59.5	59.8	8.2	8.3	12.6	12.5	247–248
9	59.2	59.5	8.2	8.3	12.9	12.8	262–263
10	59.0	58.5	8.2	8.2	13.2	13.1	257–258
11	58.8	58.4	8.2	8.2	13.5	13.4	271–272
12	58.6	58.2	8.2	8.3	13.7	13.6	>300

[a] Thin-layer chromatography (silica gel plates 60F-254, Merck) was performed in (1) chloroform–ethanol 90:10 and (2) chloroform–ethanol 95:5. The compounds were revealed by the hypochloride–starch–iodide chromatic reaction. A single spot was observed in each case with constant R_f^1 or R_f^2 of 0.55 and 0.35, respectively, in the whole series of compounds (n = 7–12). [b] Determined on a Kofler Model apparatus (Reichert, Wien); the compounds were recrystallized from acetonitrile.

Aib-OH,[62,65,66] and its mixed anhydride with pivalic acid[62] were synthesized as described. Z-(Aib)$_n$-O*t*Bu (n = 1–6),[63–65] Z-(Aib)$_n$-OH (n = 1–6),[62–65] and the corresponding oxazolones (n = 2–6)[34,62,63] have physical and analytical data in agreement with those described in the literature. A summary of the analytical data and physical properties of Z-(Aib)$_n$-O*t*Bu (n = 7–12) is reported in Table I.

Infrared Absorption. Infrared absorption spectra were recorded by using a Perkin-Elmer Model 580 B spectrophotometer equipped with a Perkin-Elmer Model 3600 IR data station. The band positions are accurate to ±1 cm^{-1}. Cells with path lengths 0.1 and 1.0 cm (with CaF_2 windows) were used for the solution measurements. Spectrograde deuteriochloroform (99.8% deuterated) was purchased from Merck. For the measurements at variable temperature a Specac Model P/N 21.000 (Analytical Accessories, Ltd., Orpington, Kent, U.K.) thermostatically controlled cell was used. Spectra were taken by using a 1.0 mm pathlength sample cell with AgCl windows. Temperature was measured directly in the sample by using a thermocouple. Because some of the bands exhibited sensitivity to humidity, the presence of which was revealed by the occurrence of significant absorptions at 3670 and 3580 cm^{-1}, great care was paid to ensure the absence of water in the solvent. The thermal stability of the urethane N-blocking group and the ester C-blocking group was checked by thin-layer chromatography after standing 60 min at 55 °C in chloroform. For the solid-state measurements the KBr disk technique was used.

^{1}H Nuclear Magnetic Resonance. The ^{1}H nuclear magnetic resonance spectra were recorded by using a Bruker WP 200 SY spectrometer. Measurements were carried out in deuteriochloroform (99.96% deuterated; Merck) and dimethyl sulfoxide (99.96%, *d*; Stohler) with tetramethylsilane as the internal standard. The free radical Tempo (2,2,6,6-tetramethylpiperidinyl-1-oxy) was purchased from Sigma.

Conformational Energy Computations. Conformational energy calculations have been performed by employing the efficient package NB/83,[67] which evaluates the conformational energy as a sum of nonbonded, electrostatic, hydrogen-bond, and intrinsic torsional contributions, as suggested by Momany et al.,[68] and taking into account the recent updating of Némethy et al.[69] The net atomic charges, as well as the geometry of the peptide, were taken from ref 12, but for the averaging of the geometrical parameters relative to the methyl groups on the C$^\alpha$.[70] After an initial search into the whole conformational space (employing a grid mesh of 10°), minimum-energy conformations were obtained in the low-energy regions by the OPT/83 package[67] using Davidon–Fletcher–Powell[71] or Newton–Raphson[72] algorithms with analytical evaluation of both the gradient and the Hessian. The precision in the determination of minima was set to about 0.1° for any of the variables. Conformational energies are expressed as $\Delta E = E - E_0$, where E_0 is the energy of the most stable conformation including variability of the N–C$^\alpha$–C′ angle. Intrinsic bending potentials have also been included in this study.

Results and Discussion

Conformational Energy Computations. It is well documented[73–75] that many of the properties of oligomers are determined by the interatomic forces within each residue of the chain. It is possible therefore to arrive at a first approximation of the most likely regular conformations of the oligomers from the (φ, ψ) energy surface for the individual residue. In the case of Aib, several theoretical studies have predicted that the conformational space is sterically restricted and low-energy conformations are found only in the region of helical structures.[3–17] We have, however, recently shown that other α,α-dialkylated α-amino acids actually prefer fully extended conformations[15,70] and X-ray data indicate that this modification is paralleled by a strong reduction of the N–C$^\alpha$–C′ angle, whereas the other intramolecular geometrical parameters remain practically unmodified.[15,32] Furthermore, IR measurements in CCl_4 suggest (although the evidence is not conclusive) the presence of some low-energy extended conformation also in the case of blocked Aib itself.[41]

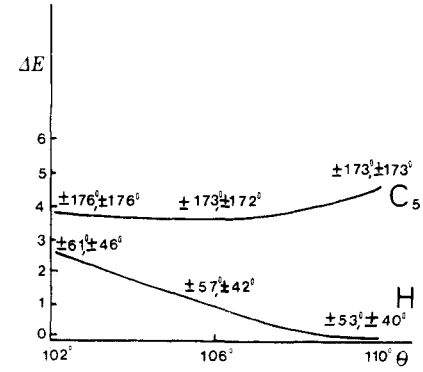

Figure 1. Conformational energy, ΔE (kcal/mol), of the fully extended (C_5) and helical (H) conformations of Ac-Aib-NHMe vs. the N–C$^\alpha$–C′ angle (ϑ). The optimized values of φ and ψ are also reported for both conformations at ϑ = 102°, 106°, and 111°.

Figure 1 shows the trend of the conformational energy computed for the extended and helical structures of blocked Aib as a function of the N–C$^\alpha$–C′ valence angle (ϑ). It is apparent that in the whole range of values considered (which covers the complete set of X-ray values for peptides) the helical structure remains the most stable, although the energy difference decreases on decreasing the N–C$^\alpha$–C′ angle. Bending contributions evaluated according to ref 76 or 77 amount to 1.1 and 0.5 kcal/mol, respectively, at N–C$^\alpha$–C′ = 102° and become negligible (<0.1 kcal/mol) in the range 107° < N–C$^\alpha$–C′ < 112°. Furthermore, the five valence angles on the C$^\alpha$ involving the C$^\beta$ atoms assume values in the range 109°–111° irrespective of the value of the N–C$^\alpha$–C′ angle. A comparison with ab initio computations for Gly and L-Ala suggests that the parameters used in the present study overestimate the relative stability of helical structures with respect to extended ones by a constant amount of about 3.5 kcal/mol.[78] Taking into account this correction, the most stable helical structure (ϑ = 111°, φ = ±53°, ψ = ±40°) still remains 0.3 kcal/mol lower in energy than the most stable extended conforma-

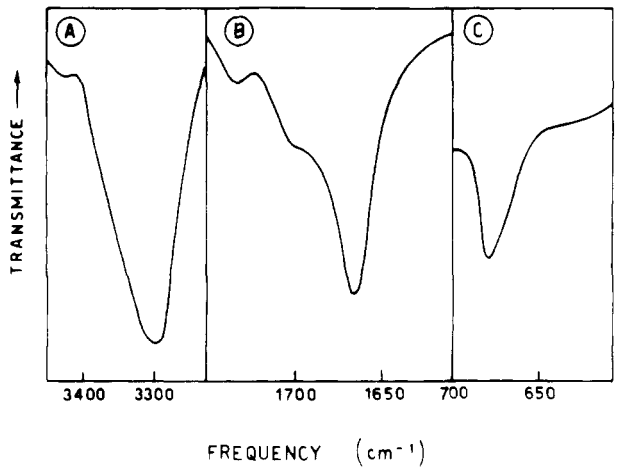

Figure 2. IR absorption spectrum of Z-(Aib)$_{12}$-O*t*Bu in the solid state: (A) 3450–3250-cm^{-1} region, (B) 1750–1600-cm^{-1} region; (C) 700–610-cm^{-1} region.

tion (ϑ = 107°, φ = 173°, ψ = 172°), but the very small energy difference becomes compatible with the detection of a nonnegligible percentage of extended structures. When the chain length is increased, ($n \geq 3$), a further stabilization is obtained only in the case of helical structures due to the formation of intramolecular H bonds between different residues, thus suggesting a shift of the conformational equilibrium toward helical structures.

As a last point we observe that the ϑ, φ, and ψ values of the most stable helix are very similar to those obtained in ref 12 for an asymmetric geometry (ϑ = 111°, φ = ±55.5°, ψ = ±40.3°). Since the contour diagram of hydrogen-bond distances in the 3_{10}- and α-helical regions in the φ, ψ map of regular oligomers depends only on the backbone geometrical parameters, also in our case the 3_{10}-helix is the preferred conformation (Figure 6 of ref 12). When the N-C$^\alpha$-C′ angle is decreased, the energy minimum moves toward φ, ψ values characteristic of the α-helix (Figure 1). We can therefore conclude that the most significant parameter in determining the preferred conformation is the N-C$^\alpha$-C′ angle.

Solid-State Conformational Analysis. We have extended the IR absorption study of the modes of folding and self-association of the Z-(Aib)$_n$-O*t*Bu peptides (already reported for the oligomers with n = 3–5)[32] to the higher oligomers (n = 6–12). The most informative frequency ranges are the following:[32,79] (i) 3450–3270 cm^{-1}, corresponding to the N-H stretching vibrations of the peptide (amide A) and urethane groups; (ii) 1800–1600 cm^{-1}, corresponding to the C=O stretching vibrations of the peptide (amide I), urethane, and ester groups; and (iii) 800–600 cm^{-1}, corresponding to the N-H out-of-plane bending mode of the peptide (amide V) and urethane groups. As an example, the spectrum of the dodecamer is shown in Figure 2.

In the 3450–3270-cm^{-1} region a band of low intensity is seen at a frequency ≥3422 cm^{-1} in all n = 6–12 oligomers, the position of which is indicative of the occurrence of free (or extremely weakly H-bonded) N-H groups. In addition, a more intense band, related to strongly H-bonded N-H groups, is visible at 3315–3298 cm^{-1}. In this spectral region a single absorption at 3275 cm^{-1} is shown by poly(Aib)$_n$,[28] whereas the corresponding absorptions of the peptaibol antibiotics alamethicin and suzukacillin fall at 3300 cm^{-1}.[80]

In the 1800–1600-cm^{-1} region three bands are seen: the weak bands at 1737–1728 and 1707–1700 cm^{-1} are assigned to absorptions of the C=O groups of free *tert*-butyl ester moieties and weakly H-bonded urethane moieties, respectively, whereas the intense band at 1664–1656 cm^{-1} is attributed to absorptions of the C=O groups of H-bonded peptide moieties. The band of the bonded C=O groups of poly(Aib)$_n$,[28] alamethicin,[80] and suzukacillin[80] appears at 1660–1652 cm^{-1}.

The characteristic feature of the spectra in the 800–600-cm^{-1} range is a relatively broad band centered near 680 cm^{-1} the intensity of which increases with increasing main-chain length. The critical chain length for the onset of this band is n = 5–6. The amide V band of poly(Aib)$_n$ is found at 694 cm^{-1},[28] whereas that of a typical α-helix is at 620–630 cm^{-1}.[79] In this region the IR spectra of the oligomers are markedly affectd by the extent of cristallinity of the compounds.

In the three regions the spectra of the higher oligomers are very similar and significantly simplified if compared with those of the lower oligomers. The IR absorption results allow us to conclude that in the solid state the Aib higher oligomers adopt an ordered secondary structure characterized by strong H bonds. As for the type of secondary structure formed, the amide I band position (≃1660 cm^{-1}) is not compatible with the onset of a β-structure (1630 cm^{-1}).[79] It is not possible to discriminate between α- and 3_{10}-helices from the spectra in the amide A and amide I regions, since the predicted frequencies are very nearly the same.[30] From an analysis of the amide V region, where significant differences between the two types of helical structure are expected,[30] evidence has been obtained for the formation of the 3_{10}-helix at the n = 5–6 level.

To ascertain unambiguously the molecular structure and the packing modes of the Aib homopeptides in the solid state, we took advantage of the high crystallinity of these compounds for an extensive single-crystal X-ray diffraction investigation. The structures of Z-(Aib)$_3$-O*t*Bu, Z-(Aib)$_4$-OH, and Z-(Aib)$_5$-O*t*Bu are characterized by the formation of (incipient) 3_{10}-helices, formed by one, two, and three intramolecular H bonds of the C_{10} type.[31-33] The same type of structure is exhibited by Tos-(Aib)$_5$-OMe (Tos = tosyl or *p*-toluenesulfonyl; OMe = methoxy).[37,39] Recently, we have been able to grow single crystals suitable for an X-ray diffraction analysis from Z-(Aib)$_8$-O*t*Bu and *p*BrBz-(Aib)$_8$-O*t*Bu (*p*BrBz = *p*-bromobenzoyl). The structure of the latter octapeptide has been solved and found to be of the 3_{10}-helical type. The details of this structure will be reported elsewhere.

Solution Conformational Analysis. The conformational preferences of the Z-(Aib)$_n$-O*t*Bu (n = 1–12) homopeptides have been investigated in a solvent of low polarity ($CDCl_3$) at various concentrations and temperatures by using IR absorption in the amide A and the amide I regions and ^{1}H NMR. The IR absorption and ^{1}H NMR data of the (n = 3–5) lower oligomers where already reported.[32,45]

The most significant IR absorption results are illustrated in Figures 3–6. Relevant conclusions are the following:

(i) Using the Mizushima's dilution technique,[81] we have been able to demonstrate that at 1.5 mM concentration intermolecular H bonding is negligible for all oligomers but the dodecamer, whereas self-association occurs at concentrations higher than 10 mM for the oligomers with n ≥ 3. In fact at low concentrations the bands at 3450–3400 cm^{-1} are assigned to the free urethane and peptide NH groups, while the bands at 3380–3317 cm^{-1} are assigned to the intramolecular H-bonded N-H groups.[32,45,50,51,81] When the concentration is increased over 10 mM, the area of the bands at 3380–3317 cm^{-1} increases (Figure 3)[44] since the broad band assigned to intermolecularly H-bonded

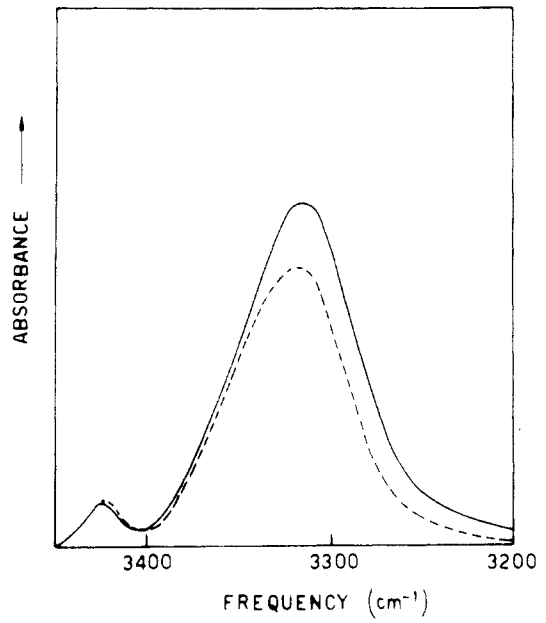

Figure 3. Concentration dependence of the NH stretching bands in the IR absorption spectrum of Z-(Aib)$_{11}$-O*t*Bu in $CDCl_3$: (—) 15 and (- - -) 1.5 mM.

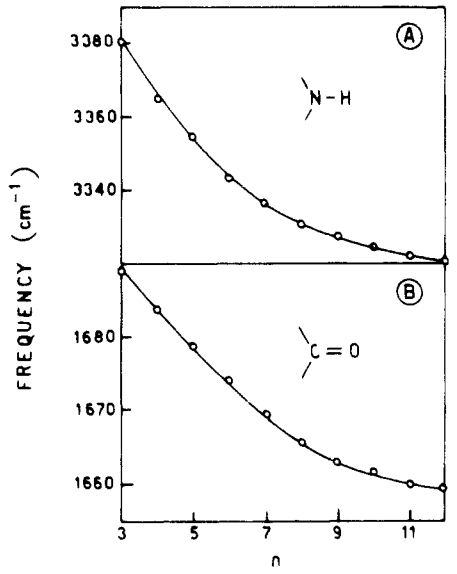

Figure 4. Frequency variation of absorption maximum of the IR absorption band in intramolecularly H-bonded peptide NH groups (A) and intramolecularly H-bonded peptide CO groups (B) vs. *n*, number of peptide residues in the homologous series Z-(Aib)$_n$-O*t*Bu (n = 3–12) in $CDCl_3$. Concentration: 1.5 mM.

N–H groups is overlapping the corresponding band of intramolecularly H-bonded N–H groups. This phenomenon becomes increasingly important as peptide chain length increases (the dodecapeptide is insoluble in $CDCl_3$ at concentrations higher than 10 mM). In this connection, it should be recalled that it is the N(1)–H that plays the role of the H-bonding donor in the self-association process of the 3_{10}-helices formed by Z-(Aib)$_n$-O*t*Bu (n = 3–5)[32] and *p*BrBz-(Aib)$_8$-O*t*Bu in the solid state.

(ii) In the absence of self-association (concentration, 1.5 mM), as the peptide chain length is enhanced, the frequencies of the absorption maxima of the stretching bands of intramolecularly H-bonded peptide N—H and C=O groups (the latter absorption[32] is seen at 1685–1659 cm^{-1}) tend to decrease (Figure 4). This variation is steeper in the range of n = 3–8, whereas significantly less pronounced in the range of n = 8–12. This finding is in favor of the conclusion that a fully developed, stable, intramolecularly

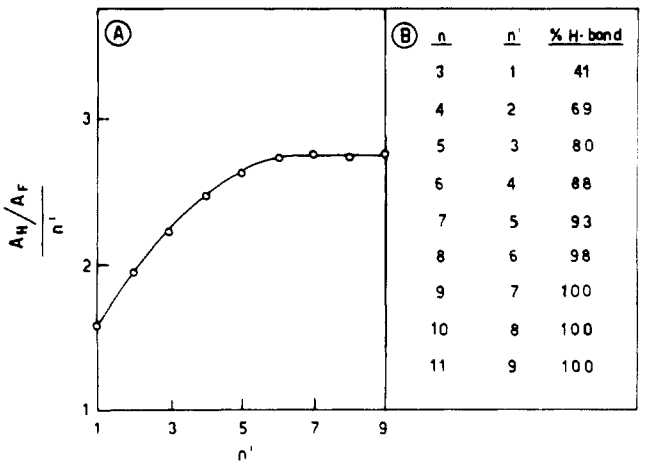

n	n'	% H-bond
3	1	41
4	2	69
5	3	80
6	4	88
7	5	93
8	6	98
9	7	100
10	8	100
11	9	100

Figure 5. (A) Plot of the A_H/A_F over n' ratios vs. n' (n = 1–9), where n' is the number of intramolecular H bonds of the 3_{10}-helices formed by the homopeptides Z-(Aib)$_n$-O*t*Bu (n = 3–11). (B) Table listing the percentages of intramolecular H bonds vs. n and n'. Solvent, $CDCl_3$; concentration, 1.5 mM.

H-bonded structure is formed at about the octamer level. The dodecamer shows the two maxima at 3320 and 1659 cm^{-1}, respectively. If these two frequencies are compared with the corresponding frequencies of the same peptide in the solid state (3298 and 1657 cm^{-1}, respectively) (Figure 2A,B), it is clear that the strong self-association effect operative in the solid state plays a significant role on the frequency of the absorption maximum of bonded peptide N–H groups, much less so on that of bonded peptide C=O groups.

(iii) In the plot of the A_H/A_F over n' as a function of n' (where A_H/A_F is the ratio of the integrated intensity of the band of H-bonded N–H groups to free N–H groups[32,45,81] and $n' = n - 2$ is the number of the intramolecular H bonds of the corresponding 3_{10}-helices) a trend parallel to the abscissa is expected when stable 3_{10}-helices are formed in the absence of self-association. Figure 5 shows that this is verified for n' = 6–9 (n = 8–11). The lower oligomers exhibit decreasing percentages of intramolecular H bonds, as peptide chain length is reduced. This percentage is still remarkably high for the oligomers from tetramer to heptamer, while clearly reduced, although still consistent, for the trimer. The A_H/A_F over n' value for the dodecamer (not reported in Figure 5) is much higher than expected, thereby confirming that this peptide is still partially self-associated at 1.5 mM. Interestingly, the results shown in Figure 4 as well as those in Figure 5 all indicate that a fully developed, stable, intramolecularly H-bonded structure (most probably a 3_{10}-helix[32]) is formed at the octamer level in the absence of self-association.

(iv) The thermal stability of the structures adopted by the oligomers with n = 3–11 in the absence of self-association is notably high, as typically shown by the amide A region of the octamer in Figure 6.

The ^1H NMR experiments on the Z-(Aib)$_n$-O*t*Bu (n = 1–12) peptides have been performed as a function of temperature (at two concentrations) (Table II), addition of the strong H-bonding acceptor solvent Me_2SO[82] (Table III) and the free radical Tempo[83] (Table III). Figure 7 graphically describes the results for the octamer.

On the basis of a comparison with model peptides[45,84,85] among the various resonances of NH protons we could assign unambiguously only those of the urethane N(1)H proton at higher fields (5.17–6.06 ppm) and the peptide N(2)H at immediately lower fields (6.29–6.92 ppm). As for the other NH protons, it is evident that the number of related peaks at lower fields (7.08–7.73 ppm) increases

Table II
NH Proton Chemical Shifts (ppm) and Their Temperature Dependencies ($\Delta\delta/\Delta T \times 10^{-3}$ ppm), in Parentheses, in the ^{1}H NMR Spectra of the Z-(Aib)$_n$-O*t*Bu (n = 1–12) Oligomers in Deuteriochloroform

n	compd concn, mM	N(1)H	N(2)H	N(3)H	N(4)H	N(5)H	N(6)H	N(7)H	N(8)H	N(9)H	N(10)H	N(11)H	N(12)H
1	18	5.40 (2.8)											
	4	5.45 (2.6)											
2	13	5.38 (2.2)	6.92 (1.2)										
	3	5.37 (1.6)	6.92 (1.3)										
3	13	5.19 (0.8)	6.49 (−2.7)	7.09 (2.8)									
	3	5.17 (0.5)	6.49 (−2.6)	7.08 (2.5)									
4	14	5.19 (3.9)	6.31 (0.5)	7.09 (3.5)	7.21 (2.6)								
	3	5.12 (3.0)	6.31 (0.9)	7.08 (3.5)	7.20 (2.5)								
5	15	5.31 (7.1)	6.30 (1.1)	7.15 (3.0)	7.27 (1.8)	7.31 (3.7)							
	4	5.24 (4.8)	6.30 (1.4)	7.18 (2.5)	7.30 (1.8)	7.37 (3.3)[a]							
6	14	5.57 (9.2)	6.38 (2.5)	7.28 (3.2)	7.36 (2.5)[a]	7.41 (4.1)[a]	7.49 (3.9)						
	1.2	5.17 (2.9)	6.31 (0.9)	7.25 (2.4)	7.34 (2.5)[a]	7.38 (2.5)[a]	7.44 (2.9)						
7	18	5.77 (10.3)	6.44 (3.0)	7.37 (2.7)[a]	7.38 (2.7)[a]	7.48 (3.4)	7.53 (33.2)	7.57 (2.8)					
	1.8	5.23 (1.1)	6.32 (1.1)	7.32 (3.1)	7.32 (3.1)	7.44 (3.5)	7.47 (3.2)	7.53 (2.7)					
8	13	5.91 (12.0)	6.54 (4.6)	7.40 (2.0)[a]	7.40 (2.0)[a]	7.51 (3.5)	7.60 (3.2)	7.60 (2.6)	7.64 (2.5)				
	1.5	5.29 (5.0)	6.36 (1.7)	7.34 (2.0)	7.35 (2.4)[a]	7.48 (4.0)[a]	7.54 (3.0)	7.57 (2.5)	7.62 (2.6)				
9	15	5.95 (12.1)	6.50 (3.7)	7.41 (1.4)[a]	7.41 (1.4)[a]	7.53 (3.5)	7.63 (3.2)	7.65 (1.9)	7.65 (1.9)	7.65 (1.9)			
	1.4	5.29 (4.5)	6.35 (1.3)	7.37 (1.9)[a]	7.37 (1.9)[a]	7.49 (3.5)	7.57 (3.2)	7.62 (2.0)	7.62 (2.0)	7.62 (2.0)			
10	16	6.06 (11.5)	6.55 (4.6)	7.42 (1.4)[a]	7.43 (1.8)[a]	7.54 (3.5)	7.67 (3.6)	7.68 (2.2)	7.68 (2.2)	7.68 (2.2)	7.71 (2.0)		
	1.5	5.36 (5.2)	6.38 (1.9)	7.38 (2.5)[a]	7.38 (2.5)[a]	7.50 (3.4)	7.58 (2.7)	7.65 (2.0)	7.65 (1.8)	7.65 (1.8)	7.69 (1.9)		
11	17	5.98 (10.3)	6.54 (3.7)	7.42 (1.2)[a]	7.43 (1.8)[a]	7.54 (3.1)	7.66 (2.8)	7.67 (1.7)	7.68 (1.8)	7.68 (1.5)	7.73 (1.7)	7.73 (1.7)	
	0.8	5.25 (3.6)	6.35 (1.0)	7.38 (2.2)[a]	7.38 (2.2)[a]	7.51 (3.4)	7.58 (2.5)	7.65 (1.7)	7.65 (1.7)	7.66 (1.7)	7.70 (2.0)	7.71 (1.9)	
12	1	5.28 (3.8)	6.35 (1.0)	7.37 (1.4)[a]	7.37 (1.4)[a]	7.51 (3.5)	7.59 (2.5)	7.66 (1.7)	7.66 (1.7)	7.66 (1.7)	7.71 (1.3)	7.71 (1.3)	7.73 (1.6)

[a] This resonance is overlapped by that of the aromatic protons of the (benzyloxy)carbonyl N-protecting group.

Table III
Variations of the Chemical Shifts of NH Protons in the ^{1}H NMR Spectra of the Z-(Aib)$_n$-O*t*Bu (n = 1–11) Oligomers as a Function of Addition of Me_2SO to the $CDCl_3$ Solutions (15 mM), $\Delta\delta/\Delta(\%Me_2SO) \times 10^3$ ppm[a]

n	N(1)H	N(2)H	N(3)H	N(4)H	N(5)H	N(6)H	N(7)H	N(8)H	N(9)H	N(10)H	N(11)H
1	-49.8 (3.1)										
2	-72.7 (4.1)	-10.3 (1.6)									
3	-93.0 (16)	-27.3 (2.7)	-9.1 (1.0)								
4	-112.5	-38.4	-15.7	-7.0							
5	-108.1 (50)	-47.5 (7.1)	-8.2 (0.7)	-5.2 (0.7)	-5.7[b]						
6	-97.5 (70)	-49.6 (11)	-5.9 (0.6)	-8.9[b]	-11.5 (1.2)	-10.6 (0.4)					
7	-89.7	-38.4	-0.4	0[b]	-2.8	-4.3	-6.2				
8	-80.8 (50)	-46.0 (15)	-0.4 (0.8)[b]	-0.4 (0.8)[b]	-3.0 (0.8)	-3.3 (1.0)	-4.0 (1.0)	-5.7 (1.0)			
9	-83.2	-47.8	0.1[b]	0.4[b]	-2.7	-3.0	-2.2	-3.2	-6.4		
10	-77.3	-43.6	0.8[b]	1.6[b]	-2.1	-0.7	-1.0	-3.4	-4.5	-3.0	
11	-72.0 (100)	-47.0 (25)	0 (0.4)[b]	1.8 (0.4)[b]	-1.9 (1.2)	-1.4 (1.0)	-1.4 (1.0)	-3.6 (1.0)	-4.6 (1.0)	-2.1 (1.0)	-1.8 (1.0)

[a] In parentheses, variations as a function of addition of Tempo ($\Delta\Delta\nu_{1/2}/\Delta(\%\text{Tempo}) \times 10^{-1}$ Hz) under the same experimental conditions. [b] This resonance is overlapped by that of the aromatic protons of the (benzyloxy)carbonyl N-protecting group.

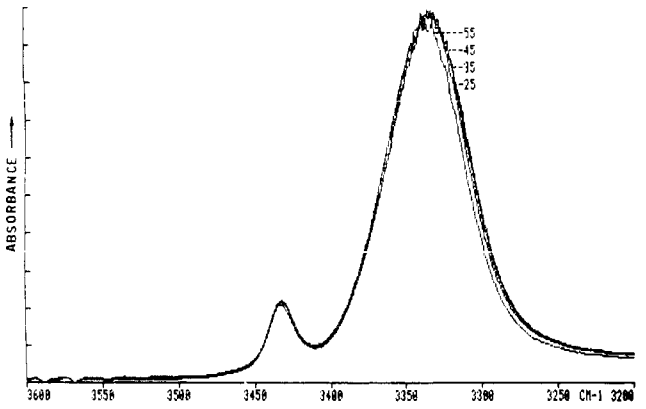

Figure 6. Temperature dependence of the stretching band of the intramolecularly H-bonded NH groups (3331 cm^{-1}) in the IR absorption spectrum of Z-(Aib)$_8$-O*t*Bu in $CDCl_3$ (concentration, 2 mM) relative to the band of free NH groups at 3427 cm^{-1}.

with increasing peptide chain length. This finding represents a preliminary indication of the involvement of these NH protons in a H-bonding scheme. It is pertinent to mention here that we number the amino acid residues as usual[45,84,85], i.e., from the N terminus of the peptide chain, so that the proton attached to the nitrogen of the N-terminal residue is labeled N(1)H.

A detailed analysis of the spectra of the homooligomers as a function of concentration (Table II) shows that an approximately 10-fold dilution (from 18–13 to 4–0.8 mM) produces a significant variation (to higher fields) of the chemical shifts of N(1)H and N(2)H protons, more evident for the urethane N(1)H.[86] This phenomenon is particularly relevant for the oligomers with $n \geq 8$, although still appreciable for the hexamer and heptamer. For the protons at lower fields, N(3)H → N(11)H, the concentration effect is negligible. The dodecamer is not sufficiently soluble in $CHCl_3$ to allow a concentration study to be performed.

Marked variations of the temperature dependencies of NH chemical shifts at the two concentrations (Table II and Figure 7A) are seen only for the urethane N(1)H protons, beginning at the tetramer level. More limited variations are observed for the peptide N(2)H protons, beginning at the hexamer level. For all other protons, N(3)H → N(11)H, the $\Delta\delta/\Delta T$ values are slightly influenced by a change in concentration. The extent of the concentration effect on the $\Delta\delta/\Delta T$ values of N(1)H protons is similar for

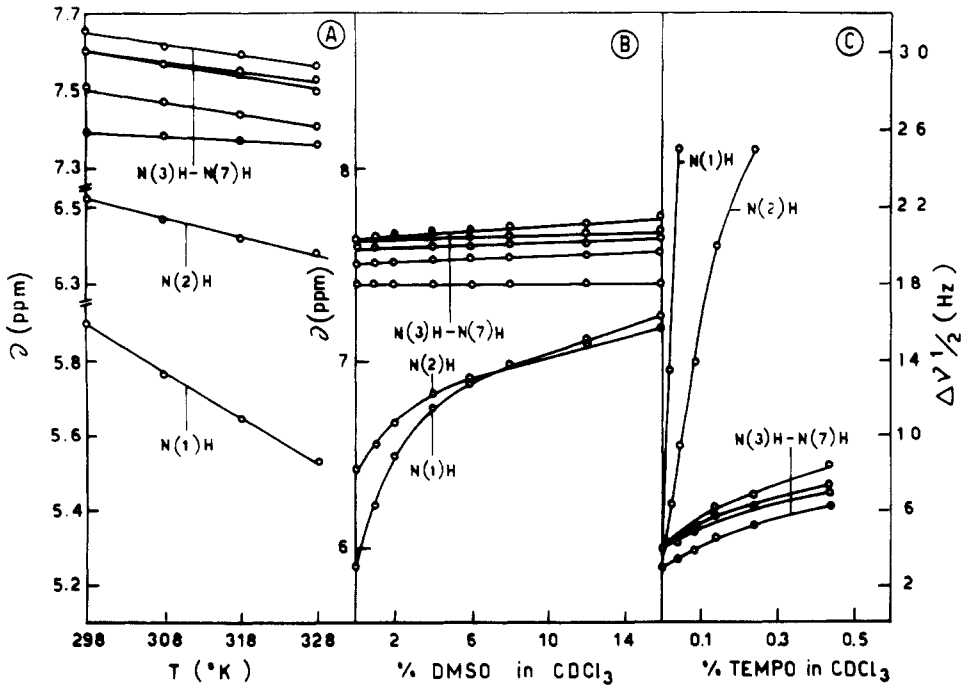

Figure 7. (A) Plot of NH chemical shifts in the ^{1}H NMR spectra of Z-(Aib)$_8$-O*t*Bu in $CDCl_3$ vs. temperature. (B) Plot of NH chemical shifts of the same peptide vs. increasing percentage of Me_2SO to the $CDCl_3$ solution (v/v). (C) Plot of the bandwidth of the NH protons of the same peptide vs. increasing percentages of Tempo (w/v) in $CDCl_3$. Concentration: 15 mM.

the oligomers with n = 8–11.

The solvent accessibilities of the NH protons of the various oligomers, indicative of a possible participation of inter- or intramolecular H bonds, have been examined as a function of addition of Me_2SO and Tempo to the $CDCl_3$ solution. As far as the addition of Me_2SO is concerned, two types of NH protons are observed:[87] the N(1)H and N(2)H protons are much more sensitive to Me_2SO than all other NH protons, N(3)H → N(11)H. In addition, the sensitivity of the N(1)H protons is notably higher than that of the N(2)H protons (Table III and Figure 7B). The variation of the chemical shifts upon addition of this strong H-bonding acceptor solvent[82] is to lower fields.[87]

A precise determination of the resonance broadening induced by the paramagnetic free radical Tempo[83] has proved difficult for some NH protons due to overlapping with resonances of the aromatic NH protons of the (benzyloxy)carbonyl N-protecting group. However, two classes of NH protons can easily be observed: the first class includes the N(1)H and N(2)H protons, the resonances of which broaden significantly upon addition of Tempo, whereas the second class includes all other NH protons, the resonances of which are only slightly sensitive to Tempo (Table III and Figure 7C).

Taking together all the ^1H NMR data, it is evident that at higher concentration (above 15 mM) the N(1)H as well as the N(2)H protons of the Z-(Aib)$_n$-O*t*Bu (n = 3–11) oligomers are involved in the intermolecular H-bonding schemes, i.e., in the self-association process, whereas all other protons form intramolecular H bonds. Self-association can be disrupted either by heating or by addition of Me_2SO and Tempo. At an approximately 10-times lower concentration, self-association is negligible for all the oligomers examined, with the single exception of the dodecamer. The intramolecular H-bonding schemes are not sensitive to changes in concentration. The intramolecular H bonds have been observed to be markedly stronger than the intermolecular H bonds, since they are stable to increasing temperature and addition of both Me_2SO and Tempo. Since all NH protons (beginning from the N(3)H proton) of the polypeptide chains of the Z-(Aib)$_n$-O*t*Bu (n = 3–12) oligomers form stable intramolecular H bonds, it may be concluded that the secondary structure adopted by the aforementioned oligomers in $CDCl_3$ is the 3_{10}-helix.

These conclusions are in agreement with those obtained from the IR measurements (described above). Finally, a comparison between solid-state and solution results leads us to conclude that the *pleionomers* from the conformationally restricted Aib residue form a (3_{10}) helical structure insensitive to environmental effects. We believe that the present results (i) represent a decisive proof in favor of the 3_{10}-helix as the preferred conformation of poly(Aib)$_n$ and (ii) are relevant to the nature of the channel formed in the membranes by the self-associated helices of the peptaibol antibiotics, whose sequence is characterized by long stretches of Aib residues.

References and Notes

(1) This work is part 121 of the series "Linear Oligopeptides". Part 120: Valle, G.; Toniolo, C.; Bonora, G. M. *Acta Crystallogr., Sect. C*, in press.
(2) (a) Institute of Organic Chemistry, University of Padua. (b) Department of Chemistry, University of Naples.
(3) Marshall, G. In "Intra-Science Chemistry Reports"; Kharasch, N., Ed.; Gordon and Breach: New York, 1971; pp 305–16.
(4) Marshall, G. R.; Gorin, F. A. In "Peptides"; Goodman, M., Meienhofer, J., Eds.; Wiley: New York, 1977; pp 84–7.
(5) Marshall, G. R.; Bosshard, H. E. *Circ. Res., Suppl. II* **1972**, *30/31*, 143.
(6) Burgess, A. W.; Leach, S. J. *Biopolymers* **1973**, *12*, 2599.
(7) Burgess, A. W.; Leach, S. J. *Biopolymers* **1973**, *12*, 2691.
(8) Burgess, A. W.; Paterson, Y.; Leach, S. J. In "Peptides, Polypeptides and Proteins"; Blout, E. R., Bovey, F. A., Goodman, M., Lotan, N., Eds.; Wiley: New York, 1974; pp 79–88.
(9) Burgess, A. W.; Paterson, Y.; Leach, S. J. *J. Polym. Sci., Polym. Symp.* **1975**, *49*, 75.
(10) Pletnev, V. Z.; Gromov, E. P.; Popov. E. M. *Khim. Prir. Soedin.* **1973**, *9*, 224.
(11) Peters, D.; Peters, J. *J. Mol. Struct.* **1982**, *86*, 341.
(12) Paterson, Y.; Rumsey, S. M.; Benedetti, E.; Némethy, G.; Scheraga, H. A. *J. Am. Chem. Soc.* **1981**, *103*, 2947.
(13) Balaram, P. In "Peptides: Structure and Function"; Hruby, V. J., Rich, D. H., Eds.; Pierce Chemical Co.: Rockford, IL, 1983; pp 477–86.
(14) Venkataram Prasad, B. V.; Balaram, P. *CRC Crit. Rev. Biochem.*, in press.
(15) Benedetti, E.; Toniolo, C.; Hardy, P.; Barone, V.; Bavoso, A.; Di Blasio, B.; Grimaldi, P.; Lelj, F.; Pavone, V.; Pedone, C.; Bonora, G. M.; Lingham, I. *J. Am. Chem. Soc.* **1984**, *106*, 8146.
(16) Venkataram Prasad, B. V.; Sasisekharan, V. *Curr. Sci.* **1979**, *48*, 517.
(17) Venkataram Prasad, B. V.; Sasisekharan, V. *Macromolecules* **1979**, *12*, 1107.
(18) Blout, E. R.; Fasman, G. D., locally cited in ref 19.
(19) Elliott, A.; Bradbury, E. M.; Downie, A. R.; Hanby, W. E. In "Polyamino Acids, Polypeptides, and Proteins"; Stahmann, M. A., Ed.; The University of Wisconsin Press: Madison, WI, 1962, pp 255.
(20) Ballard, D. G. H.; Bamford, C. H. *J. Chem. Soc.* **1958**, 355.
(21) Yamashita, T.; Isemura, T. *Bull. Soc. Chem. Jpn.* **1965**, *38*, 420.
(22) Sekiguchi, H.; Froyer, G. *J. Polym. Sci., Polym. Symp.* **1975**, *52*, 157.
(23) Froyer, G.; Sekiguchi, H. *Bull. Soc. Chim. Fr.* **1975**, 2321.
(24) Sekiguchi, H. *Pure Appl. Chem.* **1981**, *53*, 1689.
(25) Amouyal, M.; Coutin, B.; Sekiguchi, H. *J. Macromol. Sci., Chem.* **1983**, *A20*, 675.
(26) Elliott, A. *Proc. R. Soc., London Ser. A* **1954**, *226*, 408.
(27) Elliott, A.; Malcolm, B. R. *Trans. Faraday Soc.* **1956**, *52*, 528.
(28) Malcolm, B. R. *Biopolymers* **1977**, *16*, 2591.
(29) Malcolm, B. R. *Biopolymers* **1983**, *22*, 319.
(30) Krimm, S.; Owivedi, A. M. *Proc. IUPAC Macromol. Symp.* **1982**, 41.
(31) Benedetti, E.; Pedone, C.; Toniolo, C. In "Peptides 1980"; Brunfeldt, K., Ed.; Scriptor: Copenhagen, 1981; pp 619–24.
(32) Benedetti, E.; Bavoso, A.; Di Blasio, B.; Pavone, P.; Pedone, C.; Crisma, M.; Bonora, G. M.; Toniolo, C. *J. Am. Chem. Soc.* **1982**, *104*, 2437.
(33) Toniolo, C.; Bonora, G. M.; Bavoso, A.; Benedetti, E.; Di Blasio, B.; Pavone, V.; Pedone, C. *Biopolymers* **1983**, *22*, 205.
(34) Toniolo, C.; Bonora, G. M.; Crisma, M.; Benedetti, E.; Bavoso, A.; Di Blasio, B.; Pavone, V.; Pedone, C. *Int. J. Peptide Protein Res.* **1983**, *22*, 603.
(35) Valle, G.; Bonora, G. M.; Toniolo, C. *Can. J. Chem.*, in press.
(36) Valle, G.; Bonora, G. M.; Toniolo, C. *Gazz. Chim. Ital.*, in press.
(37) Shamala, N.; Nagaraj, N.; Balaram, P. *J. Chem. Soc., Chem. Commun.* **1978**, 996.
(38) Nair, C. M. K.; Vijayan, M. *Acta Crystallogr., Sect. B* **1980**, *36*, 1498.
(39) Rao, Ch. P.; Shamala, N.; Nagaraj, R.; Rao, C. N. R.; Balaram, P. *Biochem. Biophys. Res. Commun.* **1981**, *103*, 898.
(40) Venkataram Prasad, B. V.; Balaram, P. In "Conformation in Biology"; Srinivasan, R., Sarma, R. H., Eds.; Adenine Press: Guilderland, NY, 1983; pp 133–9.
(41) Aubry, A.; Protas, J.; Boussard, G.; Marraud, M.; Néel, J. *Biopolymers* **1978**, *17*, 1693.
(42) Mayr, W.; Jung, G.; Strahle, J. *Liebigs Ann. Chem.* **1980**, 715.
(43) Van Roey, P.; Smith, G. D.; Balasubramanian, T. M.; Marshall, G. R. *Acta Crystallogr., Sect. C* **1983**, *39*, 894.
(44) Wilkening, R. R.; Stevens, E. S.; Bonora, G. M.; Toniolo, C. *J. Am. Chem. Soc.* **1983**, *105*, 2560.
(45) Bonora, G. M.; Mapelli, C.; Toniolo, C.; Wilkening, R. R.; Stevens, E. S. *Int. J. Biol. Macromol.* **1984**, *6*, 179.
(46) Bonora, G. M.; Toniolo, C.; Di Blasio, B.; Pavone, V.; Pedone, C.; Benedetti, E.; Lingham, I.; Hardy, P. *J. Am. Chem. Soc.*, **1984**, *106*, 8152.
(47) Paterson, Y.; Stimson, E. R.; Evans, D. J.; Leach, S. J.; Scheraga, H. A. *Int. J. Peptide Protein Res.* **1982**, *20*, 468.
(48) Dorlet, C.; Toussaint, A. *Bull. Soc. Chim. Belg.* **1964**, *73*, 127.
(49) Marraud, M.; Néel, J. *C. R. Seances Acad. Sci., Ser. C* **1974**, *278*, 1015.
(50) Pulla Rao, Ch.; Nagaraj, R.; Rao, C. N. R.; Balaram, P. *FEBS Lett.* **1979**, *100*, 244.
(51) Pulla Rao, Ch.; Nagaraj, R.; Rao, C, N. R.; Balaram, P. *Biochemistry* **1980**, *19*, 425.

(52) Pulla Rao, Ch.; Balaram, P.; Rao, C. N. R. *Biopolymers* **1983**, *22*, 2091.
(53) Toniolo, C. *CRC Crit. Rev. Biochem.* **1980**, *9*, 1.
(54) Zahn, H.; Gleitsmann, G. B. *Angew. Chem.* **1963**, *75*, 772.
(55) Nagaraj, R.; Balaram, P. *Acc. Chem. Res.* **1981**, *14*, 356.
(56) Mathew, M. K.; Balaram, P. *Mol. Cell. Biochem.* **1983**, *50*, 47.
(57) Jung, G.; Brückner, H.; Schmitt, H. In "Structure and Activity of Natural Peptides"; Voelter, G., Weitzel, G., Eds.; de Gruyter: Berlin, 1981; pp 75-114.
(58) Jung, G.; Becker, G.; Schmitt, H.; Voges, K. P.; Boheim, G.; Griesbach, S. In "Peptides: Structure and Function"; Hruby, V. J., Rich, D. H., Eds.; Pierce Chemical Co.: Rockford, IL, 1983; pp 491-4.
(59) Hall, J. E.; Balasubramanian, T. M.; Hing, A.; Marshall, G. R. In "Peptides: Structure and Function"; Hruby, V. J., Rich, D. H., Eds.; Pierce Chemical Co.: Rockford, IL, 1983; pp 487-90.
(60) Roeske, R. W.; Kennedy, S. J. In "Chemistry and Biochemistry of Amino Acids, Peptides, and Proteins"; Weinstein, B., Ed.; Marcel Dekker: New York, 1983; Vol. 7, pp 205-65.
(61) Fox, R. O.; Richards, F. M. *Nature (London)* **1982**, *300*, 325.
(62) Leplawy, M. T.; Jones, D. S.; Kenner, G. W.; Sheppard, R. C. *Tetrahedron* **1960**, *11*, 39.
(63) Jones, D. S.; Kenner, G. W.; Preston, J.; Sheppard, R. C. *J. Chem. Soc.* **1965**, 6227.
(64) Ali, M. Y.; Dale, J.; Titlestad, K. *Acta Chem. Scand.* **1973**, *27*, 1509.
(65) Leibfritz, D.; Haupt, E.; Dubischar, N.; Lachmann, H.; Dekonomopulos, R.; Jung, G. *Tetrahedron* **1982**, *38*, 2165.
(66) McGahren, W. J.; Goodman, M. *Tetrahedron* **1967**, *23*, 2017.
(67) Barone, V.; Lelj, F., to be submitted for publication.
(68) Momany, F. A.; McGuire, R. F.; Burgess, A. W.; Scheraga, H. A. *J. Phys. Chem.* **1979**, *79*, 2361.
(69) Némethy, G.; Pottle, M. S.; Scheraga, H. A. *J. Phys. Chem.* **1983**, *87*, 1883.
(70) Barone, V.; Bavoso, A.; Grimaldi, P.; Lelj, F.; Pavone, V.; Pedone, C. *Biopolymers*, submitted.
(71) (a) Davidon, W. C. *Comput. J.* **1968**, *10*, 406. (b) Fletcher, R., Powell, M. J. D. *Comput. J.* **1963**, *6*, 163.
(72) Harwell Library Routine No. VA11A.
(73) Scheraga, H. A. *Chem. Rev.* **1971**, *71*, 195.
(74) Ramachandran, G. N.; Sasisekharan, V. *Adv. Protein Chem.* **1968**, *23*, 283.
(75) Brant, D. A.; Flory, P. J. *J. Am. Chem. Soc.* **1965**, *87*, 2791.
(76) Weiner, S. J.; Kollman, P. A.; Case, D. A.; Singh, U. Ch.; Ghio, C.; Alagona, G.; Profeta, S., Jr.; Weiner, P. *J. Am. Chem. Soc.* **1984**, *106*, 765.
(77) Levitt, M.; Lifson, Sh. *J. Mol. Biol.* **1969**, *46*, 269.
(78) Scarsdale, J. N.; Van Alsenoy, C.; Klimkowski, V. J.; Schafer, L.; Momany, F. A. *J. Am. Chem. Soc.* **1983**, *105*, 3438.
(79) Miyazawa, T. In "Poly-α-Amino Acids"; Fasman, G. D., Ed.; Marcel Dekker: New York, 1967; pp 69.
(80) Jung, G.; König, W. A.; Leibfritz, D.; Ooka, T.; Janko, K.; Boheim, G. *Biochim. Biophys. Acta* **1976**, *433*, 164.
(81) Mizushima, S.; Shimanouchi, T.; Tsuboi, M.; Souda, R. *J. Am. Chem. Soc.* **1952**, *74*, 270.
(82) Martin, D.; Hauthal, G. In "Dimethyl Sulfoxide"; Van Nostrand-Reinhold: Wokingham, England, 1975.
(83) Kopple, K. D.; Schamper, T. J. *J. Am. Chem. Soc.* **1972**, *94*, 3644.
(84) Pysh, E. S.; Toniolo, C. *J. Am. Chem. Soc.* **1977**, *99*, 6211.
(85) Stevens, E. S.; Sugawara, W.; Bonora, G. M.; Toniolo, C. *J. Am. Chem. Soc.* **1980**, *102*, 7048.
(86) Iqbal, M.; Balaram, P. *Biopolymers* **1982**, *21*, 1427.
(87) Pitner, T. P.; Urry, D. W. *J. Am. Chem. Soc.* **1972**, *94*, 1399.

Molecular Level Model for Motion and Relaxation in Glassy Polycarbonate

Alan A. Jones

Department of Chemistry, Clark University, Worcester, Massachusetts 01610.
Received July 11, 1984

ABSTRACT: A local chain motion is proposed for the low-temperature loss peak in glassy polycarbonate: namely, a correlated conformational interchange between two neighboring carbonate units. One carbonate unit starts with a trans-trans conformation and the other with a cis-trans conformation. The interchange is produced by a rotation about one of the CO bonds in each of the carbonate units. The cis-trans conformation diffuses down the chain composed of largely trans-trans units by the repeated action of this process. The phenylene group attached to the other side of the carbonate unit from the rotating CO bond undergoes a π flip as rotation about the CO bond occurs though intermolecular couplings in the bulk polymer may also link the π flips to the interchange. This motion is consistent with existing solid-state proton, carbon, and deuterium line shape data on the phenylene group. It also agrees with the presence of a substantial dielectric and dynamical mechanical loss peak linked in time to the occurrence of π flips. This motion produces a volume fluctuation by translation of the bisphenol A unit between the rearranging carbonate units; and this volume fluctuation can diffuse down the polymer chain as the cis-trans conformation diffuses. Diffusion of a change in backbone shape and a volume fluctuation down the polymer chain is a process which could initiate the rapid reduction of a macroscopic strain.

The local chain dynamics of glassy polycarbonate has intrigued many investigators over the past 25 years. Traditional experiments probing dielectric relaxation[1-8] and dynamic mechanical relaxation[6-13] below the glass transition indicated large-scale motion with very broad loss peaks at low temperatures (the γ relaxation). These experiments were not suitable for defining the specific geometry of the motions in polycarbonate (Figure 1) though certain implications from studies of a variety of structural analogues[7,8,13] did provide useful information in developing proposals for motions. Wide-line NMR studies[14,15] also observe relaxation effects below the glass transition; but the lack of structural specificity produced only general conclusions comparable to the dielectric and dynamic mechanical work.

Recently, more sophisticated solid-state NMR line shape studies have provided some very detailed geometric information. The first definitive line shape result[16] was obtained on a structural analogue of BPA polycarbonate which contained only phenylene protons (Figure 2). The proton spectrum showed the undiminished persistence of a dipolar splitting between adjacent phenylene protons up to the glass transition. This implied that the virtual bond corresponding to the phenylene group could not be reorientating in space. It did allow for either translation of the phenylene group or reorientation of the phenylene group about the C_1C_4 axis. This conclusion was later confirmed for the polycarbonate in Figure 1 through observations on a partially deuterated form.[17]

Subsequent attention centered on the phenylene group

0024-9297/85/2218-0902$01.50/0